

UNCLASSIFIED TR-116

ARO-15862.21-M

DAAG29-79-C-0121

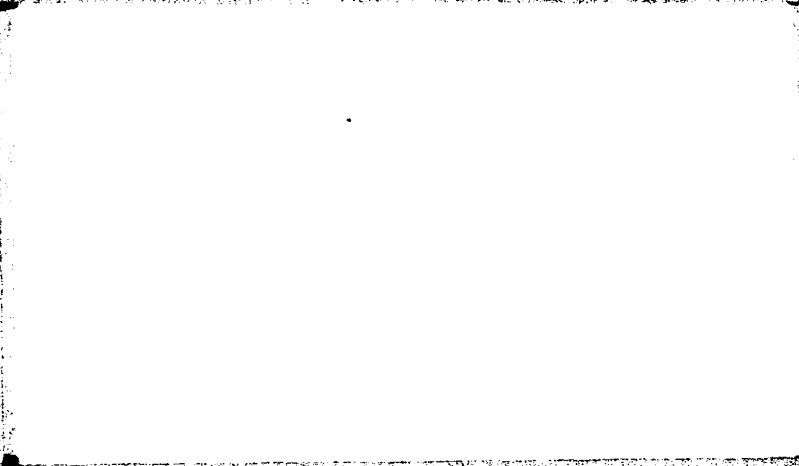
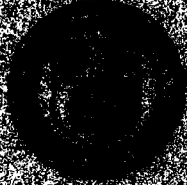
NL

1. Δ_1

END
DATE
FILED
at 1:50 PM
DTIC

AD A090776

LEVEL II



THE FULL COPY

Approved for Release by NSA on 08-12-2013 pursuant to E.O. 13526

DTIC
OCT 23 1980
A

This document has been approved for public release and sale in its entirety without restriction.

FAST DEFLAGRATION WAVES

Technical Report No. 116

D.S. Stewart & G.S.S. Ludford

July 1980

Accession For	
NTIS GRA&I	<input checked="checked" type="checkbox"/>
DTIC TAB	<input type="checkbox"/>
Unannounced	<input type="checkbox"/>
Justification	
By	
Distribution/	
Availability Codes	
Dist	Avail and/or Special
A	

U.S. Army Research Office
Research Triangle Park, NC 27709

Contract No. DAAG29-79-C-0121

Cornell University
Ithaca, NY 14853

Approved for public release; distribution unlimited

Contents

	Page
1. Introduction	1
2. The governing equations	2
3. Activation-energy asymptotics	3
4. Fast deflagration waves	4
5. Small heat release: $\beta \ll 1$	9
6. The combustion approximation	11
7. Very slow deflagrations	14
8. Application of these results for large θ	19
Appendix I: $Pr, Le \neq 1$	22
Appendix II: The exponential tail	28
References	29
Table 1	30
Captions	31
Figures 1-5	33

The findings in this report are not to be construed as an official Department of the Army position, unless so designated by other authorized documents.

1. Introduction

The analysis of steady plane deflagration waves invariably starts with the combustion approximation where it is assumed that the Mach number, i.e. the flame speed divided by a characteristic sound speed, is vanishingly small. The momentum equation then implies that the pressure is nearly constant while the thermal and mechanical descriptions of the wave decouple, so that the task of solving for the structure is greatly simplified. Even then explicit formulas can only be obtained in the limit of large activation energy.

We are currently interested in describing, by means of activation-energy asymptotics as far as possible, the transition from deflagration to detonation in gases. One of the first steps in such a theory is to analyze deflagration waves whose Mach numbers are not vanishingly small. Pressure variations cannot be neglected and hence the momentum equation must be retained in the description of the structure. We will show, in the present paper, that the method of activation-energy asymptotics gives an analytic description of these fast deflagrations, i.e. deflagrations travelling at speeds greater than those justifying the use of the combustion approximation. In addition we examine the limit of vanishingly small Mach number to shed light on the nature of the combustion approximation.

The main result is that the Mach number of a fast deflagration wave is determined (implicitly) by the flame temperature, a parameter of the mixture. But an interesting feature is a secondary reaction over an exponentially long tail in which the small amount of reactant escaping the initial flame is finally consumed. In addition, for small Mach numbers we find a hydrodynamic adjustment layer behind the flame and another possible wave, neither of which can be detected by the combustion approximation. In short, we have extended the classical work of Bush and Fendell (1970) to finite Mach numbers, and uncovered the existence of very slow deflagration waves.

2. The governing equations

The governing equations of a plane, steady deflagration express the balances of mass, momentum, energy and species. In deriving the equations used here certain assumptions are made, the most important being: steadiness, one-step reaction, Arrhenius kinetics, ideal gas, Newtonian fluid, Fick's diffusion law, equal specific heats and constant material properties. See Buckmaster & Ludford (1981).

In what follows ρ, v, T and Y are respectively the dimensionless density, gas velocity, temperature and mass fraction of the deficient reactant (if there is more than one). The density and temperature in the quiescent conditions upstream are taken as units so that the dependent variables ρ, v, T, Y tend to 1, 0, 1, Y_∞ as $s \rightarrow -\infty$, where s denotes distance from the flame. The distance unit is the preheat thickness $\lambda/c_p M$, where λ and c_p are respectively the thermal conductivity and specific heat of the fluid; and M is the mass flux, the velocity unit being the flame speed. The other important parameters that appear are defined in Table 1.

The Prandlt and Lewis numbers will both be set equal to one, solely to simplify our discussion. Prandlt and Lewis numbers different from unity are discussed in Appendix I.

The equations of steady plane combustion can then be shown to reduce to

$$\gamma M_0^2 dV/ds = \gamma M_0^2 (V-1) + (TV^{-1}-1), \quad (1)$$

$$d\tau/ds = d^2\tau/ds^2 + \alpha Y e^{-\theta/T}, \quad (2)$$

$$T = \tau - (\gamma-1)M_0^2 V^2/2, \quad (3)$$

$$\tau + \alpha Y = 1 + \beta + (\gamma-1)M_0^2/2 \quad \text{with } \beta = \alpha Y_\infty, \quad (4)$$

$$\rho V = 1 \quad \text{with} \quad V = v + 1. \quad (5)$$

The perfect-gas law serves to define the pressure, which has been eliminated. In the present formulation, V and τ will be the basic variables, the temperature T and mass fraction Y serving as auxiliary variables defined by (3) and (4) respectively. Thus equations (1) and (2) are to be solved under the conditions that $V, \tau \rightarrow 1, 1 + (\gamma - 1)M_0^2/2$ as $s \rightarrow -\infty$ and that the solution is bounded as $s \rightarrow +\infty$. Equation (5) just defines the density. The singular nature of equation (1) as $M_0 \rightarrow 0$ leads to the adjustment layer mentioned in the Introduction (cf. Secs. 5 and 6).

3. Activation-energy asymptotics

We seek a solution of equations (1)-(4) in the distinguished limit

$$D = C\theta^2 \exp(\theta/T_*) \quad \text{with } \theta \rightarrow \infty. \quad (6)$$

Here the constants C and T_* are supposed given; their determination for an actual mixture is considered in Sec. 8. The connection between the wave speed and the mass flux M is made explicit by writing

$$M = mM_0 \quad (7)$$

(m is the so-called acoustic impedance). Thus the reaction term in equation (2) appears as

$$\Lambda Y e^{-\theta/T} = C\theta^2 Y \exp[\theta(1/T_* - 1/T)] / m^2 M_0^2 \quad (8)$$

As $\theta \rightarrow \infty$, there are three possible regimes. In regions where $T < T_*$, the reaction term is exponentially small and hence negligible compared to algebraic perturbations; the chemistry is frozen. In regions where $T > T_*$,

the reaction term is unbounded unless Y is zero to all order in θ^{-1} ; equilibrium prevails. Finally, the regions in which $T - T_\infty = O(\theta^{-1})$ are flame sheets, found to be characterized by a reaction/diffusion balance. Equilibrium regions will in fact only occur in the limit of the combustion approximation.

4. Fast deflagration waves

We now determine the structure of fast deflagration waves. The flame sheet is located at $s = 0$ and on either side the chemistry is frozen, as we shall see. Expanding the variables in the form

$$u = u_0 + \theta^{-1} u_1 + \dots \quad (9)$$

and assuming Y is zero to leading order in the burnt region shows that

$$\tau_0 = 1 + \beta e^s + (\gamma-1)M_0^2/2, \quad Y_0 = Y_\infty(1-e^s) \quad \text{for } s < 0, \quad (10)$$

and

$$\tau_0 = 1 + \beta + (\gamma-1)M_0^2/2, \quad Y_0 = 0 \quad \text{for } s > 0. \quad (11)$$

The solution for V_0 requires some discussion. On both sides of the flame sheet V_0 is governed by (1) where V and T are taken to leading order and T_0 is defined in terms of V_0 and τ_0 by (3). For $s > 0$ the fixed points of equation (1) are

$$V_\pm = [(\gamma M_0^2 + 1) \pm \sqrt{(1-M_0^2)^2 - 2(\gamma+1)M_0^2\beta}]/(\gamma+1)M_0^2 \quad (12)$$

which shows that the restriction

$$(1-M_0^2)^2/2(\gamma+1)M_0^2 \geq \beta \quad (13)$$

must be placed on M_0 for a given heat release β . Equality corresponds to the Chapman-Jouget deflagration, so that the present theory will yield Mach numbers in the range

$$0 \leq M_O^2 < M_{OCJ}^2 = [1 + (\gamma+1)\beta - \sqrt{(1+(\gamma+1)\beta)^2 - 1}]. \quad (14)$$

Integrating (1) for $s > 0$ shows that

$$\frac{2\gamma}{\gamma+1} \frac{1}{(V_+ - V_-)} \ln \frac{|V_O - V_+|^{\frac{V_+}{V_-}}}{|V_O - V_-|^{\frac{V_-}{V_+}}} = s + c \quad (15)$$

where c is a constant. Since $V_+ - V_-$ is positive, $V_O \rightarrow V_-$ as $s \rightarrow +\infty$, which is appropriate for weak deflagrations.

For $s < 0$, we cannot integrate equation (1) analytically without further assumption because T_O contains e^s . Nevertheless its integration with $V = 1$ for $s = -\infty$ determines the value $V_O = V_*(M_O^2) < V_-$ at $s = 0$. Determination follows from the saddle-point nature of the cold-boundary point in the τ, V -plane; the inequality results from $dV/ds \geq 0$ for $s > 0$, not a simple result to verify. As a consequence T_O decreases from its value T_* at the flame because τ_O is constant.)

Since V_* is determined by the integration for $s < 0$, the constant c in (15) is fixed and

$$T_* = T_O(0) = 1 + \beta + (\gamma-1)M_O^2(1-V_*^2)/2. \quad (16)$$

Thus the flame temperature is determined as a function of the flame speed, i.e. M_O^2 . If T_* is a monotonically decreasing function of M_O^2 , which is usually found to be the case for reasonable values of β, γ, Pr , then there is a unique M_O^2 for the given T_* in the definition (6) of D . A typical plot of M_O^2 vs. T_* is shown in Fig. 1a.

Note that no discussion of higher-order terms or structure of the flame sheet is necessary to determine the flame speed. Only the minimal assumption of continuity across the flame sheet is made. The analysis is distinctly different from that for M_O small (using the combustion approximation), where a discussion of the structure (and hence higher-order terms) is needed to determine M_O .

On either side of the flame sheet the perturbations of τ and Y are

$$\tau_1 = \tau_- e^s \text{ for } s < 0, \quad \tau_1 = \tau_+ \text{ for } s > 0 \text{ and } Y_1 = -\tau_1/\alpha; \quad (17)$$

while V_1 satisfies

$$\gamma M_0^2 dV_1/ds = V_1(M_0^2 - T_0/V_0^2) + \tau_1/V_0 \text{ for all } s \neq 0. \quad (18)$$

The integration constants τ_{\pm} are determined by the flame-sheet structure, as we shall see next. Note that τ_+ is not zero: an $O(\theta^{-1})$ amount of reactant escapes burning and passes downstream where, over exponentially large distances, it is finally consumed. The process is described in Appendix II.

To investigate the structure, let

$$z = \theta s \quad (19)$$

and consider the expansions

$$\tau = 1 + \theta + (\gamma - 1)M_0^2/2 + \theta^{-1}\tilde{\tau}_1(z) + \dots, \quad V = V_* + \theta^{-1}\tilde{V}_1(z) + \dots, \quad Y = \theta^{-1}\tilde{Y}_1(z) + \dots \quad (20)$$

$$T = T_* + \theta^{-1}T_1(z) + \dots$$

Then we easily find

$$\tilde{V}_1 = \delta z + V_1(0) \text{ with } \delta = V_* - 1 + (T_*/V_* - 1)\gamma M_0^2, \quad (21)$$

where $V_1(0)$ is at this stage an unidentified constant. However, it follows by matching that V_1 in the outer expansions is continuous across the flame sheet, so that $V_1(0)$ is in fact the common value there (hence the notation). The solution of equation (18) is determined, once τ_{\pm} are found, by the upstream condition $V_1(-\infty) = 0$. Clearly the upstream solution, and hence the constant $V_1(0)$ in (21), depends on τ_- while the downstream solution depends on both τ_+ and τ_- .

The $\tilde{\tau}_1$ -problem now becomes

$$\left. \begin{aligned} d^2 \tilde{\tau}_1 / dz^2 &= \tilde{\lambda} \tilde{\tau}_1 e^{\tilde{\tau}_1 / T_*^2} \text{ with } \tilde{\tau}_1 = \tau_1 - (\gamma-1) M_0^2 V_* [\delta z + V_1(0)] \\ \text{and } \tilde{\lambda} &= C/m^2 M^2, \\ \tilde{\tau}_1 &= \beta z + \tau_- + o(1) \text{ as } z \rightarrow -\infty, \quad \tilde{\tau}_1 = \tau_+ + o(1) \text{ as } z \rightarrow +\infty \end{aligned} \right\} \quad (22)$$

where the boundary conditions are obtained by matching. A transformation reduces (22) to a structure problem discussed by Liñán [1974]. Let

$$\left. \begin{aligned} \sigma &= -\tilde{\tau}_1 / T_*^2, \quad w = (\gamma-1) M_0^2 V_* \delta / \beta, \\ \zeta &= \beta z / T_*^2 + \beta V_1(0) / \delta T_*^2 + (1/w) \ln \{ \beta^2 / 2 \tilde{\lambda} T_*^4 \}; \end{aligned} \right\} \quad (23)$$

then

$$\left. \begin{aligned} 2d^2 \sigma / d\zeta^2 &= \sigma \exp \{-\sigma - w\zeta\}, \\ \sigma &= -\zeta - \tau_- / T_*^2 + V_1(0) / \beta T_*^2 + (1/w) \ln \{ \beta^2 / 2 \tilde{\lambda} T_*^4 \} + o(1) \text{ as } \zeta \rightarrow -\infty, \\ \sigma &= -\tau_+ / T_*^2 + o(1) \text{ as } \zeta \rightarrow +\infty. \end{aligned} \right\} \quad (24)$$

Liñán found (numerically) that, whenever w is less than $1/2$, a solution of the equation (24a) is uniquely determined by the weaker boundary conditions

$$d\sigma/d\zeta \rightarrow -1 \text{ as } \zeta \rightarrow -\infty, \quad d\sigma/d\zeta \rightarrow 0 \text{ as } \zeta \rightarrow +\infty. \quad (25)$$

By adjusting the (finite) starting point for the left boundary condition he was able to satisfy the right boundary condition, and thereby approximate the parameters

$$\sigma_-(w) = \lim_{\zeta \rightarrow -\infty} (\sigma + \zeta), \quad \sigma_+(w) = \lim_{\zeta \rightarrow +\infty} \sigma. \quad (26)$$

For $0 < w < 1/2$, as is the case here, σ_+ was found to be positive while $\sigma_- \rightarrow 1.344$, $\sigma_+ \rightarrow 0$ as $w \rightarrow 0$. [Proof that w is less than $1/2$ has been given by Lu & Ludford (1981).] It follows that for our problem

$$-\tau_-/T_*^2 + V_1(0)\beta/\delta T_*^2 + w^{-1} \ln\{\beta^2/2\tilde{\Lambda}T_*^4\} = \sigma_-, \quad -\tau_+/T_*^2 = \sigma_+ \quad (27)$$

are thereby determined.

To complete the determination of τ_{\pm} we must calculate $V_1(0)$ in terms of τ_- , which requires the equation (18) for V_1 in $s < 0$ to be integrated under the condition $V_1(-\infty) = 0$. The solution is

$$V_1 = \tau_- \Omega(s), \quad \text{with} \quad \Omega(s) = \frac{\exp(f(s))}{\gamma M_0^2} \int_{-\infty}^s \exp \frac{(s'-f(s'))}{\gamma M_0^2 V_0(s')} ds' \quad (28)$$

where
$$f(s) = \frac{1}{\gamma M_0^2} \int_0^s (M_0^2 - T_0/V_0^2) ds';$$

and hence

$$V_1(0) = \tau_- \Omega(0). \quad (29)$$

We now have asymptotic approximations to order θ^{-1} in the three regions, for any set of parameter values $C, T_*, m, \beta, \gamma, Y_{-\infty}$. To summarize, these approximations are determined as follows. First τ_0 , and hence Y_0 , is determined by solving the reactionless equation (2) on either side of the flame sheet assuming continuity across the sheet and $Y_0 = 0$ for $s > 0$. The solution is given by equations (10) and (11). V_0 is then determined by integrating equations (1) to leading order, numerically for $s < 0$ and analytically [equation (15)] for $s > 0$. The temperature follows from equation (3), depending in particular on M_0 . Setting

$T_0(0) = T_*$ then fixes the flame speed (represented by M_0) as a function of the flame temperature T_* , according to equation (16). Fig. 2a is the result of carrying out these steps for one particular set of parameters.

The approximation to the next higher order is obtained by solving for V_1 and τ_1 in the outer regions ($s \lesssim 0$), see equations (17) and (28), and determining the corresponding constants $\tau_1, V_1(0)$ through the relations (27) and (29). These relations are obtained from the structure of the flame sheet and explicit integration of the equation for V_1 in $s < 0$, respectively.

Explicit analytical results can be obtained when the heat release is small, in which case all variables stay close to their values upstream. Note that this limit can be taken for any value of M_0 , i.e. it is quite independent of the combustion approximation $M_0 \rightarrow 0$.

5. Small heat release: $\beta \ll 1$

The smallness of the heat release may be due either to a small heat of reaction or to a small amount of reactant. It enables analytical expressions to be developed for the results in Sec. 4 that otherwise have to be derived by numerical integration.

We write

$$V_0 = 1 + \beta V' + \dots, \quad \tau_0 = 1 + (\gamma-1)M_0^2/2 + \beta \tau' + \dots \quad (30)$$

so that

$$Y_0 = \beta(1-\tau')/\dots, \text{ and } T_0 = 1 + \beta[\tau' - (\gamma-1)M_0^2 V'] + \dots \quad (31)$$

Then

$$\tau' = \begin{cases} e^s & \text{for } s < 0, \\ 1 & \text{for } s > 0 \end{cases} \quad (32)$$

and

$$(33) \quad \gamma M_0^2 dV'/ds = -(1-M_0^2)V' + \tau'. \quad (33)$$

The solution which vanishes at $s = -\infty$ and is continuous at $s = 0$ is

$$V' = \begin{cases} [1+(\gamma-1)M_0^2]^{-1}e^s & \text{for } s < 0, \\ [1-M_0^2]^{-1}\{1-\gamma M_0^2[1+(\gamma-1)M_0^2]^{-1}e^{-(1-M_0^2)s/\gamma M_0^2}\} & \text{for } s > 0. \end{cases} \quad (34)$$

Note that when M_0 is small a rapid hydrodynamic adjustment takes place behind the flame sheet, given by the exponential term in (34 b). The combustion approximation takes the thickness of this Mach layer [which is a consequence of the singular nature of the differential equation (33) as $M_0 \rightarrow 0$] to be zero.

Consider the distinguished limit

$$T_* = 1 + \beta t_*, \quad C = \beta^2 \tilde{C} \quad \text{with } \beta \rightarrow 0. \quad (35)$$

For t_* in an appropriate interval, T_* is attainable, i.e. it lies between the upstream temperature and the adiabatic flame temperature; and τ_* , obtained from equation (27 a), remains bounded as $\beta \rightarrow 0$. As explained in Sec. 4, in order to determine the wave speed, we calculate the temperature at $s = 0$ and set it equal to T_* . Here the relation between T_* and M_0^2 becomes explicit, namely

$$t_* = 1/[1+(\gamma-1)M_0^2] \quad (36)$$

In particular, as T_* approaches the adiabatic flame temperature T_a , i.e. $t_* \rightarrow 1$, the flame speed vanishes, i.e. $M_0^2 \rightarrow 0$. The restriction (13) on the heat release is not violated unless M_0^2 becomes close to $M_{OCJ}^2 = 1 + O(\beta^{1/2})$, thus t_* varies between 1 and $1/\gamma < 1$.

To complete the analysis we calculate the θ^{-1} perturbations explicitly. Details are omitted; suffice it to say that, to leading order in β , we find

$$\delta = \beta/\gamma, w = [(\gamma-1)/\gamma]M_0^2, \quad \Omega(s) = [1/(1+(\gamma-1)M_0^2)]e^s \quad (37)$$

so that

$$v_1(0) = \tau_-/[1+(\gamma-1)M_0^2], \quad (38)$$

where, from equation (27 a),

$$\tau_- = \frac{1+(\gamma-1)M_0^2}{(\gamma-1)(1-M_0^2)} \left[\sigma_{-\infty} + \frac{\gamma}{(\gamma-1)M_0^2} \ln \left(\frac{m^2 M_0^2}{2\tilde{C}} \right) \right] \quad (39)$$

In short, the solution to $O(\theta^{-1})$, both inside and outside the flame sheet, is explicitly determined once \tilde{C} and t_* are specified. The flame speed is determined by t_* alone, while \tilde{C} only enters at the perturbation. This means that changing C affects the structure of the flame (corresponding to a slight translation) and hence the perturbation it produces upstream and downstream, but not its velocity.

6. The Combustion Approximation

The limit $M_0 \rightarrow 0$ must be examined carefully. But, before doing so, we shall review the basic results of activation-energy asymptotics in the combustion approximation.

The combustion approximation is the limit $M_0 \rightarrow 0$ with θ fixed. The activation-energy limit $\theta \rightarrow \infty$ is then used to analyze the resulting equations. Thus $\lim_{\theta \rightarrow \infty} \lim_{M_0 \rightarrow 0}$ is obtained in contrast to $\lim_{M_0 \rightarrow 0} \lim_{\theta \rightarrow \infty}$ which will be obtained from the above analysis. The pre-exponential factor C in the Damköhler number is assumed to be such that $\tilde{A} = C/m^2 M_0^2$ is $O(1)$.

To all orders in θ^{-1} , equations (1-5) with $M_0 = 0$ are correct to leading order in a M_0^2 -expansion. We find immediately

$$T = \tau = V, T + \alpha Y = 1 + \beta = T_a \quad (40)$$

to all orders in θ^{-1} ; and the leading order result

$$T_0 = \begin{cases} 1 + \beta e^s & \text{for } s < 0, \\ 1 + \beta & \text{for } s > 0. \end{cases} \quad (41)$$

Standard flame-sheet analysis yields the structure problem (22) which, with $\tilde{\tau}_1, T_*$ replaced by \tilde{T}_1, T_a and $M_0 = 0$, becomes

$$d^2 \tilde{T}_1 / dz^2 = \tilde{\Lambda} \tilde{T}_1 e^{\tilde{T}_1 / T_a^2} \quad \text{with} \quad \tilde{\Lambda} = \zeta / m^2 M_0^2 \quad (42)$$

$$\tilde{T}_1 = \beta z + \tau_- + o(1) \quad \text{as } z \rightarrow -\infty, \quad \tilde{T}_1 = \tau_+ + o(1) \quad \text{as } z \rightarrow +\infty.$$

Clearly, τ_+ is zero; otherwise the differential equation is not consistent with the boundary condition at $z = +\infty$. A first integral

$$(d\tilde{T}_1 / dz)^2 = 2T_a^4 [1 + (\tilde{T}_1 / T_a^2 - 1)e^{\tilde{T}_1 / T_a^2}] \quad (43)$$

is obtained by using the requirement $\tau_+ = 0$. The boundary condition at $z = -\infty$ will then be satisfied only if

$$\tilde{\Lambda} = \beta^2 / 2T_a^4, \text{ i.e. } DM^{-2} = -\beta^2 \theta^2 e^{\theta / T_a} / 2T_a^4. \quad (44)$$

A further integration using the same condition yields

$$\beta z - \tau_- = T_a^2 \int_{-\infty}^{\tilde{T}_1 / T_a^2} \{[1 - (t-1)e^t]^{-1/2} - 1\} dt + \tilde{T}_1. \quad (45)$$

Thus, while the constant τ_+ is zero, τ_- is undetermined; its definition corresponds to locating an origin for the flame structure to $O(\theta^{-1})$. For the structure to exist, $\tilde{\Lambda}$ must have the value (44), corresponding to a definite distinguished limit for D as $M_0 \rightarrow 0$.

Returning to the fast deflagration with $\theta \rightarrow \infty$, we now let $M_0 \rightarrow 0$. First note from the discussion in Sec. 4 that $M_0 \rightarrow 0$ as $T_* \rightarrow T_a$: the limit of vanishingly small flames speeds corresponds to flame temperatures T_* indefinitely close to the adiabatic flame temperature T_a .

The only point at which there is difficulty in the limit is the unbounded term

$$w^{-1} \ln \{ \beta^2 / 2 \tilde{\Lambda} T_*^4 \} \quad (46)$$

in the formula (27). If, however, we set

$$\tilde{\Lambda} = \beta^2 / 2 T_*^4, \text{ i.e. } C = \beta^2 m M_0^2 / 2 T_*^4, \quad (47)$$

corresponding to

$$D = \beta^2 m^2 M_0^2 (T_*) \theta^2 \exp(\theta / T_*) / 2 T_*^4, \quad (48)$$

the term disappears and no difficulty remains. We have therefore constructed a family of asymptotic solutions, parametrized by T_* , which is uniformly valid in the interval

$$T_* \ll T_* \leq T_a. \quad (49)$$

Moreover, the member $T_* = T_a$ of this family is one of the solutions obtained by the combustion approximation.

Other uniformly valid families can be obtained by taking $\bar{\Lambda} = (\theta^2/2T_*^4)[1 + M_0^2(T_*)f(T_*)]$ with f arbitrary. This would add a factor $1 + M_0^2(T_*)f(T_*)$ to the right-hand side of (48) and change τ_- by an amount depending on T_* . Because of the exponential in the formula (48), any two such families produce the same finite D for values of T_* within $O(\theta^{-1})$ of each other. The corresponding members are therefore identical except for τ_- , a change which corresponds to translation of the wave by an $O(\theta^{-1})$ amount. The two members corresponding to $T_* = T_a$ differ in the same manner, reflecting the indeterminacy noted above for solutions under the combustion approximation.

When T_a is excluded from the T_* -interval a much larger class of uniformly valid families of solutions, all identical under translations, can be obtained by taking $\bar{\Lambda}$ to be an arbitrary function of T_* , again because of the exponential in D . Any such family which is not of the earlier type breaks down as $T_* \rightarrow T_a$ because the term (46) becomes unbounded in the limit, suggesting that there are other solutions when M_0 is small, characterized by perturbations that are large compared to θ^{-1} .

We turn now to these solutions of our general equations, finally demonstrating that they do not survive the combustion approximation. It is therefore not surprising that they have escaped detection before.

7. Very Slow Deflagrations

We now consider the distinguished limit

$$D = C\theta^2 \exp(\theta/T_*), \quad T_* = T_a - g(\theta)t_* \quad \text{with } \theta \rightarrow \infty, \quad (50)$$

where $g(\theta)$ is a positive gauge function large compared to θ^{-1} and t_* is $O(1)$. We anticipate $M_0^2 = kg(\theta)$, with $k = O(1)$ positive, and look

for expansions of the form

$$u = u_0 + g(\theta)u_g + \theta^{-1}u_1 + \dots \quad (51)$$

upstream and downstream of the flame. Thus the leading-order terms are given by formulas (10) and (11) with $M_0^2 = 0$ and $V_0 = T_0 = \tau_0$. The g -perturbations are then found by assuming continuity of T_g and τ_g (but not V_g) from one side to the other, assumptions that can be justified by considering the structure of the sheet. Thus

$$\left. \begin{aligned} \tau_g &= (\gamma-1)k/2 + [\tau_{g\infty} - (\gamma-1)k/2]e^s, \quad V_g = \tau_g - (\gamma-1)kV_0^2/2 \quad \text{for } s < 0, \\ \tau_g &= \tau_{g\infty}, \quad V_g = \tau_{g\infty} - (\gamma-1)kT_a^2/2 + \gamma k \beta T_a \quad \text{for } s > 0, \end{aligned} \right\} \quad (52)$$

where $\tau_{g\infty}$ is an as yet undetermined constant. As expected from the discussion in Sec. 5, V_g is discontinuous across the flame sheet so that a Mach layer is required. We easily find the modification

$$V_g = \tau_{g\infty} - (\gamma-1)kT_a^2/2 + \gamma k \beta T_a [1 - \exp(-s/\gamma k T_a g)] \quad \text{for } s > 0, \quad (53)$$

which makes the necessary adjustment on a scale $s = O(g)$, much larger than that of the flame sheet. The θ^{-1} -perturbations are found to be

$$\tau_1 = V_1 = \tau_- e^s \quad \text{for } s < 0; \quad \tau_1 = V_1 = \tau_+ \quad \text{for } s > 0, \quad (54)$$

where τ_{\pm} have to be determined.

To fix the constants $\tau_{g\infty}, \tau_{\pm}$ we must discuss the structure of the flame sheet, where as usual the coordinate $z = s/\theta$ is appropriate. The equations for the g -perturbations require their constancy through the flame sheet, so that the expansions there are written

$$V = T_a = g\tilde{v}_{g*} + \theta^{-1}\tilde{v}_1 + \dots, \tau = T_a + g\tilde{\tau}_{g*} + \theta^{-1}\tilde{\tau}_1 + \dots, \quad (55)$$

in terms of which

$$\tilde{T}_{g*} = \tilde{\tau}_{g*} - (\gamma-1)kT_a^2/2, \quad -\alpha\tilde{Y}_{g*} = \tilde{\tau}_{g*} - (\gamma-1)k/2 \quad (56)$$

according to the relations (3) and (4).

We first show that \tilde{Y}_{g*} must be zero. Assuming $\tilde{Y}_{g*} \neq 0$ and following the steps leading to the structure problem (22) shows that a balanced equation for $\tilde{\tau}_1$ can only be obtained if

$$g = T_a^2 \ln \theta / (t_* + \tilde{T}_{g*}) \theta. \quad (57)$$

The corresponding structure problem is

$$\left. \begin{aligned} d^2\tilde{\tau}_1/dz^2 &= A e^{\tilde{\tau}_1/T_a^2} \quad \text{with} \quad A = -\alpha\tilde{Y}_{g*} \quad C/km^2, \\ d\tilde{\tau}_1/dz &\rightarrow \beta + o(1) \quad \text{as} \quad z \rightarrow -\infty, \quad d\tilde{\tau}_1/dz \rightarrow o(1) \quad \text{as} \quad z \rightarrow +\infty. \end{aligned} \right\} \quad (58)$$

Clearly the boundary condition at $z = +\infty$ can only be satisfied if $A = 0$.

Thus the assumption $\tilde{Y}_{g*} \neq 0$ is incorrect and we must have

$$\tilde{Y}_{g*} = 0, \quad \tilde{\tau}_{g*} = (\gamma-1)k/2, \quad \tilde{T}_{g*} = -k\hat{t} < 0, \quad (59)$$

$$\text{where } \hat{t} = (T_a^2 - 1)(\gamma-1)/2.$$

Balancing the $\tilde{\tau}_1$ -equation with $\tilde{Y}_{g*} = 0$ leads to a different condition on g , namely

$$(C/m^2 kg) \exp\{\theta g(t_* - kt)/T_a^2\} = \beta^2/2T_a^4, \quad (60)$$

the $\tilde{\tau}_1$ -structure being precisely that of the combustion approximation.

Now we choose g to be the solution of

$$e^{-\theta g} = g, \quad (61)$$

thereby obtaining a positive gauge function solely dependent on θ with the property $1 \gg g(\theta) \gg \theta^{-1}$. Then equation (60) becomes

$$(C/m^2 k) \exp\{\theta g[(t_* - k\hat{t})/T_a^2 + 1]\} = \beta^2/2T_a^4, \quad (62)$$

from which θ disappears if

$$k = (t_* + T_a^2)/\hat{t}, \text{ i.e. } M_O^2 = (t_* + T_a^2)g/\hat{t}. \quad (63)$$

This determines M_O^2 as a (linear) function of t_* .

We are therefore considering a family of solutions for which

$$C = \frac{\beta^2 m^2 (t_* + T_a^2)}{2T_a^4 \hat{t}}, \text{ i.e. } D = \frac{\beta^2 m^2 \theta^2}{2T_a^4} \frac{(t_* + T_a^2)}{\hat{t}} \exp\left[\frac{\theta}{T_a - t_* g(\theta)}\right]. \quad (64)$$

The family is parameterized by t_* which, since M_O^2 is positive, cannot be less than $t_* = -T_a^2$; so that the present theory is uniformly valid in the interval

$$-T_a^2 \leq t_* \leq t_{*0} < \infty \text{ for any } t_{*0}. \quad (65)$$

Elimination of t_* and neglect of a term $O(\theta g^2)$ in the exponential yields

$$D = \frac{\beta^2 m^2 \theta^2}{2T_a^4} M_O^2 \exp[\theta/(T_a - M_O^2 \hat{t})] \quad (66)$$

9 Other uniformly valid families can be obtained by taking

$$e^{-\theta g} = \alpha g \quad (67)$$

which multiplies D by a factor α . Because of the exponential, any two such families produce the same D for values of t_* within $O(\theta^{-1}g^{-1})$ of each other, so corresponding members are identical.

The wave speeds exhibited by (63) are vanishingly small in the limit $\theta \rightarrow \infty$, i.e. much smaller than those corresponding to the combustion approximation (which was shown in Sec. 6 to make correct predictions for M_0 small but finite as $\theta \rightarrow \infty$.) Thus the solutions in this section are very slow deflagrations.

Now we shall demonstrate that the existence of these other solutions cannot be detected by the combustion approximation, whose equations were mentioned at the beginning of Sec. 6. With the distinguished limit and the expansions of the present section, it can be shown that the flame-sheet perturbation \tilde{T}_{g*} must again be zero and that the structure problem is (42) with

$$\tilde{\Lambda} = (C/m^2 kg) \exp\{\theta g t_*/T_a^2\}. \quad (68)$$

As usual, $\tilde{\Lambda}$ is found to be equal to $\beta^2/2T_a^4$; and that result together with (61) leads to the analog of (62), i.e.

$$(C/m^2 k) \exp[\theta g(t_*/T_a^2 + 1)] = \frac{\beta^2}{2T_a^4}, \quad (69)$$

where the choice (61) is again made for g .

To eliminate θ we must set

$$t_* = -T_a^2, \quad (70)$$

thereby losing t_* as a parameter, and then

$$C = (\beta/2T_a^4)km^2, \quad (71)$$

so that the solutions are now parameterized by $k = M_0^2/g$ directly. The corresponding D is (66) with $\hat{t} = 0$ which may be rewritten

$$D = \frac{\beta^2 m^2 \theta^2}{2T_a^4} \exp(\theta/T_a) \quad (72)$$

on neglect of a term $O(\theta g^2)$ in the exponential. But this formula is the same as (44); we have merely reproduced the results of Sec. 6, which hold for small M_0 up to $O(1)$ on the θ -scale, in the limit $M_0^2 = O(g)$.

Note that the only difference between formulas (66) and (72) is the presence of the term $\hat{t}M_0^2$, which results from the momentum equation neglected in the combustion approximation.

8. Application of these results for large θ

The mathematical analysis provides an asymptotic solution when the Damköhler number has the form (6) with C and T_* specified. In practice, however, D and θ (large but finite) are given instead of C and T_* , which must now be calculated from the formulas (47) and (48). Sec. 4 can then be expected to give an approximate solution, provided θ is large. The calculation of T_* is illustrated in Fig. 3, which graphs D as a function of T_* in a typical case. Note that D cannot exceed a certain value corresponding to $T_* = T_{*CJ}$ (if a steady solution is to exist). As $\theta \rightarrow \infty$ this upper bound increases indefinitely, so that for very large θ effectively any value of D leads to a steady deflagration. As D becomes small, $T_* \rightarrow T_a$ and the solution obtained through the combustion approximation is recovered.

The procedure is particularly transparent when the heat release is small. Then, according to formula (36),

$$M_o^2(T_*) = \frac{T_a - T_*}{(\gamma - 1)(T_* - 1)}, \quad (73)$$

and the restriction that $0 \leq M_o^2 < M_{oCJ}^2$ requires that

$$T_{*CJ} = 1 + \beta/\gamma < T_* \leq T_a. \quad (74)$$

Thus

$$D = \frac{\beta^2 m^2}{2(\gamma - 1)T_*^4} \frac{T_a - T_*}{(T_* - 1)} \theta^2 \exp(\theta/T_*), \quad (75)$$

which clearly leads to a curve of the form shown in Fig. 3, the maximum value of D being

$$\frac{\beta^2 m^2 \theta^2}{2(1 + \beta/\gamma)^4} \exp[\theta(1 + \beta/\gamma)]. \quad (76)$$

The results in Sec. 7 show that there is another possibility for each value of D . The calculation of t_* from the equation (64b) for large θ (g having been determined from equation (61)) is illustrated in Fig. 5. The formulas of Sec. 6 can then be expected to provide an approximate solution. Note that the second solution exists whatever the value of D , the wave speed (on the scale of $g^{1/2}$) increasing monotonically from 0 to ∞ as D does so.

Thus we have shown that, for a given D in an appropriate range, there are in fact two distinct wave speeds, one for fast deflagrations as predicted by (48) and illustrated for small heat release by equations (73) and (75), and one corresponding to very slow deflagrations as predicted by equation (66).

In the $D/m^2, M_0^2$ -plane both branches tend to the single curve (44) obtained by the combustion approximation, as $M_0^2 \rightarrow 0$. A typical plot of D/m^2 versus M_0^2 is shown in Fig. 5.

The existence of two wave speeds has been known for some time, albeit in association with heat loss under the combustion approximation. Indeed Spalding and Yamlu (1959) have reported experiments, involving heat loss, in which two wave speeds were found. More recently, Buckmaster (1976) described the slower of the two waves in the limit of vanishingly small heat loss. (The faster wave tends to the familiar deflagration wave with $T_* = T_a$, described in Sec. 6 for $\theta \rightarrow \infty$.) However, a description of the very slow waves under adiabatic conditions has apparently not been given before.

Appendix I: Pr, Le \neq 1

The assumptions of Prandtl and Lewis numbers equal to one were made for simplicity and are not essential. Here we give the changes that are required when we relax those assumptions.

The governing equations for general Pr, Le become

$$\gamma M_o^2 \text{Pr} dV/ds = \gamma M_o^2 (V-1) + TV^{-1} - 1 \quad (77)$$

$$dT/ds + (\gamma-1)TV^{-1}dV/ds = \gamma d^2T/ds^2 \quad (78)$$

$$+ \text{Pr}\gamma(\gamma-1)M_o^2(dV/ds)^2 + \alpha\gamma Y \Lambda e^{-\theta/T}$$

$$dY/ds = \text{Le}^{-1}d^2Y/ds^2 - \Lambda Y e^{-\theta/T} \quad (79)$$

Equations (77) - (79) and equation (5) under the assumptions listed in Sec. 2 are the original equations that equations (1) - (4) were derived from. By suitable combination of equation (77) and (78) one can show that τ as defined by (3) satisfies

$$\frac{d\tau}{ds} = \frac{d^2\tau}{ds^2} + (\text{Pr}-1)(\gamma-1)M_o^2 \frac{d^2(V^2/2)}{ds^2} + \alpha\Lambda Y e^{-\theta/T}, \quad (80)$$

and from (80) and (79) $H = \tau + \alpha Y$ satisfies

$$H = 1 + \beta + (\gamma-1)M_o^2/2 + \frac{d}{ds} \{ (H-\tau)(\text{Le}^{-1}-1) + (\text{Pr}-1)(\gamma-1)M_o^2V^2/2 \} \quad (81)$$

The simplification given by the dual assumption that $\text{Pr} = \text{Le} = 1$ is now obvious, equations (80) and (81) reducing to (2) and (4) respectively. Assuming the Prandtl and Lewis numbers to be unity surely leads to great simplification which motivated the form of our original discussion, but generally the variables τ and H offer no advantage over the original variables T and Y which we now will use in the following.

Reactionless equations for the $O(1)$ terms and $O(\theta^{-1})$ perturbations are to be subject to appropriate conditions at $s = -\infty$ and a set of jump conditions, denoted by

$$[u] = u_+ - u_- , \quad (82)$$

derivable from a flame-sheet analysis. The leading order conditions are

$$\left. \begin{aligned} [T_0] = [V_0] = [Y_0] = [dV_0/ds] = [dT_0/ds + \alpha Le^{-1} dY_0/ds] = 0 \\ T_0 = T_* \text{ at } s = 0 \text{ and } Y_0 = 0 \text{ for } s > 0 . \end{aligned} \right\} \quad (83)$$

The solution of the leading-order problem for a given value of M_0^2 determines the function $T_* = T_*(M_0^2)$ as in Sec. 4.

Similarly we find conditions on the $O(\theta^{-1})$ perturbations to be

$$\left. \begin{aligned} [V_1] = [T_1 + \alpha Le^{-1} Y_1] = 0 \\ [dV_1/ds] = [T_1]/\gamma M_0^2 Pr V_* , \quad [dT_1/ds + \alpha Le^{-1} dY_1/ds] = (1/\gamma - Le)[T_1] . \end{aligned} \right\} \quad (84)$$

The structure problem in the flame sheet corresponding to (22), now written in terms of \tilde{T}_1 , becomes

$$\left. \begin{aligned} \frac{d^2 \tilde{T}_1}{dz^2} = -\tilde{\Lambda} \alpha \tilde{Y}_1 e^{\tilde{T}_1/T_*^2} , \quad \tilde{T}_1 + \alpha Le^{-1} \tilde{Y}_1 = (dT_0/ds_+)z + T_{1+} + \alpha Le^{-1} Y_{1+} \\ \tilde{T}_1 \rightarrow (dT_0/ds_-)z + T_{1-} \text{ as } z \rightarrow -\infty , \quad \tilde{T}_1 \rightarrow (dT_0/ds_+)z + T_{1+} \text{ as } z \rightarrow +\infty . \end{aligned} \right\} \quad (85)$$

And as before (85) can be transformed into Liñán's problem (24) to be solved under conditions (26) with w specified as

$$w = - (dT_0/ds_+) / (dT_0/ds_- - dT_0/ds_+) ; (dT_0/ds_- - dT_0/ds_+) = \beta . (86)$$

Solution of Liñán's problem then fixes the constants Y_{1-} , Y_{1+} (analogous to τ_+ , τ_- in Sec. 4), as

$$Y_- = Le T_*^2 (\Omega + \sigma_-) / \alpha , \quad Y_+ = Le T_* \sigma_+ / \alpha \quad \left. \vphantom{\begin{matrix} Y_- \\ Y_+ \end{matrix}} \right\} (87)$$

with
$$\Omega = 1/w [T_{1+}/T_*^2 + \sigma_+ - \ln(\beta^2 / 2 \Lambda Le T_*^4)]$$

The general problem as outlined is numerical; but the limit of small heat release yields explicit formulas, as it does in Sec. 5. To all orders in β the solution for Y_0 is given as

$$Y_0 = Y_{-\infty} (1 - e^{Le s}) \text{ for } s < 0 , \quad Y_0 = 0 \text{ for } s > 0 . (88)$$

Equations (77) and (78), with the reaction term set equal to zero are to be solved subject to the required jump conditions. Expanding V_0 and T_0 as

$$V_0 = 1 + \beta v' + \dots , \quad T_0 = 1 + \beta T' + \dots , (89)$$

then v' and T' satisfy

$$\begin{aligned} dv'/ds &= [(\gamma M_0^2 - 1)v' + T'] / Pr \gamma M_0^2 , \\ d^2 T'/ds^2 &= [(\gamma - 1)dv'/ds + dT'/ds] / \gamma \end{aligned} \quad \left. \vphantom{\begin{matrix} dv'/ds \\ d^2 T'/ds^2 \end{matrix}} \right\} (90)$$

subject to

$$\begin{aligned} v' , \quad T' &\rightarrow 0 \text{ as } s \rightarrow -\infty , \text{ bounded as } s \rightarrow +\infty , \\ [v'] &= [T'] = 0 , \quad [dT'/ds] = -1 . \end{aligned} \quad \left. \vphantom{\begin{matrix} v' \\ T' \end{matrix}} \right\} (91)$$

For $0 \leq M_0^2 < 1$ we easily find

$$\left. \begin{aligned} \left(\frac{v'}{T'} \right) &= \frac{\lambda_2}{(\lambda_2 - \lambda_1)(1 - M_0^2)} \left(\frac{1}{\gamma \lambda_1 - 1} \right) e^{\lambda_1 s} \quad \text{for } s < 0, \\ \left(\frac{v'}{T'} \right) &= \frac{1}{1 - M_0^2} \left\{ \left(\frac{1}{1 - \gamma M_0^2} \right) + \frac{\lambda_1}{(\lambda_2 - \lambda_1)} \left(\frac{1}{\gamma \lambda_2 - 1} \right) e^{\lambda_2 s} \right\} \quad \text{for } s > 0, \end{aligned} \right\} (92)$$

where

$$\lambda_1, \lambda_2 = \{ [\gamma M_0^2 - 1 + \text{Pr} M_0^2] \pm \sqrt{[\gamma M_0^2 - 1 + \text{Pr} M_0^2]^2 + 4(1 - M_0^2)\text{Pr}\gamma M_0^2} \} / 2\text{Pr}\gamma M_0^2. \quad (93)$$

λ_1 and λ_2 have the properties:

$$\left. \begin{aligned} \lambda_1 &\sim 1, \quad \lambda_2 \sim -1/\gamma M_0^2 \text{Pr} \quad \text{as } M_0^2 \rightarrow 0, \\ \lambda_1 &\sim (\gamma - 1 + \text{Pr})/\gamma \text{Pr}, \quad \lambda_2 \sim -(1 - M_0^2)/(\gamma - 1 + \text{Pr}) \quad \text{as } M_0^2 \rightarrow 1. \end{aligned} \right\} (94)$$

Setting $T_0(0)$ equal to T_* of the definition (35) now shows that

$$t_* = \frac{(\gamma - 1)\lambda_2}{(\lambda_2 - \lambda_1)(1 - M_0^2)(\gamma \lambda_1 - 1)}, \quad (95)$$

which reduces to the formula (36) for $\text{Pr} = 1$. As there $t_* \rightarrow 1$, i.e. $T_* \rightarrow T_a$ as $M_0^2 \rightarrow 0$.

These formulas determine M_0 and the combustion field to leading order for arbitrary values of Pr and Le when the heat release is small. Since λ_1 is positive and λ_2 is negative for $M_0^2 < 1$, the result (92) shows that the velocity v' increase monotonically up to the flame and beyond, ultimately attaining the value $v'(\infty) = 1/(1 - M_0^2)$. On the other hand the temperature increases up to the flame but then decreases to its final value $T'(\infty) = (1 - \gamma M_0^2)/(1 - M_0^2)$. The temperature and velocity profiles are therefore qualitatively unchanged from those for $\text{Pr} = 1$. See Fig. 2a, b in Sec. 4. However the pressure field, determined by the perturbation

$$p' = T' - v' \quad (96)$$

is sensitive to the value of the Prandlt number. The pressure p' is zero as $s = -\infty$ and reaches a negative final value $p'(\infty) = -\gamma M_0^2 / (1 - M_0^2)$. In between, it may or may not have a (positive) maximum depending on whether $T'(0)$ is greater or less than $v'(0)$. For $Pr = 1$, they are equal so that the effect can be explicitly exhibited by taking Pr close to one. Thus we evaluate

$$p'(0) = \frac{\gamma \lambda_2 (1 - \lambda_1)}{(1 - M_0^2) (\lambda_2 - \lambda_1) (\gamma \lambda_1 - 1)} \quad (97)$$

for

$$\lambda_1 \sim 1 - \frac{(Pr-1)(\gamma-1)M_0^2}{\gamma M_0^2 + 1 - M_0^2} \quad \text{and} \quad \lambda_2 \sim - \frac{(1-M_0^2)}{\gamma M_0^2} \quad (98)$$

to obtain

$$p'(0) \sim \frac{\gamma M_0^2 (Pr-1)}{\gamma M_0^2 + 1 - M_0^2} \quad (99)$$

For $Pr > 1$ there is a pressure spike at the flame, whereas for $Pr < 1$ the decrease is monotonic with s from $-\infty$ to $+\infty$. Presumably there is a similar effect when the heat release is not small.

The discussion for very slow deflagrations found in Sec. 7 can also be generalized for $Pr, Le \neq 1$. Again the starting point is equations (77)-(79). Considering the distinguished limit given by (50) and allowing $M_0^2 = kg(\theta)$, the analysis $Pr, Le \neq 1$ follows precisely as in Section 7 in that we must consider outer regions $s < 0, s > 0$ and a velocity adjustment in the $O(g)$ Mach layer behind the flame sheet. The detailed solution to $O(g)$ is more complicated than that presented in Sec. 7, involving terms that vanish when $Pr = 1$, but is obtained in a straightforward fashion.

Consideration of the flame structure requires as before that $\tilde{Y}_{g*} = 0$ and thus equation (60) again holds with the right-hand side replaced with

$$\beta^2 / 2T_a^4 Le \quad (100)$$

Following the remaining arguments in Sec. 7 we find the only change is the form of D parameterized by t_* which becomes

$$D = \frac{\beta m^2 \theta^2}{2T_a^4 Le} \frac{(t_* + T_a^2)}{\hat{t}} \exp\left[\frac{\theta}{T_a - t_* g(\theta)}\right] \quad (101)$$

Appendix II: The Exponential Tail

It was shown in Sec. 4 that for any non-zero Mach number, the combustion field is comprised of a frozen region upstream and a flame sheet followed by a frozen downstream region where the temperature decreases from T_* . Thus reactant escapes from the flame in an amount measured by the perturbation $\sigma_+ = -\tau_+/T_*^2 = \alpha Y_+/T_*^2 \geq 0$. (Note that the partial burning exhibited here holds for all non-zero wave speeds, since Linán's problem controls the structure. In the limit $M_0^2 \rightarrow 0$, as in Sec. 7, $Y_+ \rightarrow 0$.) Because of this non-zero reactant fraction there must be further burning beyond, albeit exponentially weak, so as to take the reaction to completion.

Consider the expansions

$$\left. \begin{aligned} V &= V_\infty + 1/\theta V_1 + \dots, \quad \tau = \tau_\infty + 1/\theta \tau_1 + \dots; \quad T = T_\infty + 1/\theta T_1 + \dots \\ \text{where} \quad V_\infty &= V_- , \quad \tau_\infty = 1 + \beta + (\gamma-1)M_0^2/2 , \quad T_\infty = 1 + \beta + (\gamma-1)M_0^2(1-V_-^2) \end{aligned} \right\} (102)$$

and the variable

$$\eta = \Lambda e^{-\theta/T_\infty} s . \quad (103)$$

Since $T_\infty < T_*$, and Λ has the form implied by (8), $\Lambda e^{-\theta/T_\infty}$ is exponentially small compared to θ^{-1} . Hence the derivative in equation (1) is negligible to all orders in θ^{-1} and we find from (1), (3) and (4) that

$$V_1 = T_1 (V_\infty/T_\infty - \gamma M_0^2 V_\infty^2) , \quad T_1 = \tau_1 - (\gamma-1)M_0^2 V_\infty V_1 , \quad \tau_1 = -\alpha Y_1 . \quad (104)$$

Eliminating V_1 and T_1 in favor of τ_1 now shows that

$$\left. \begin{aligned} \frac{d\tau_1}{d\eta} &= -\tau_1 \exp(\hat{\alpha}\tau_1) \quad \text{with} \quad \hat{\alpha} = \frac{1}{T_\infty^2} \left(\frac{T_\infty - \gamma M_0^2 V_\infty}{T_\infty - M_0^2 V_\infty} \right), \\ \tau_1 &= -T_\infty^2 \sigma_+ \quad \text{at} \quad \eta = 0 \end{aligned} \right\} \quad (105)$$

is the problem for τ_1 in $\eta \geq 0$. (The boundary condition is obtained by matching with the burnt region immediately following the flame.)

An explicit solution can be given in terms of the exponential integral function $E_1(z) = \int_z^\infty e^{-t}/t dt$. Thus

$$\left. \begin{aligned} E_1(-\hat{\alpha}\tau_1) - E_1(\hat{\alpha}\sigma_+) &= \eta \quad \text{for} \quad \hat{\alpha} > 0, \\ \tau_1 &= -\sigma_+ e^{-\eta} \quad \text{for} \quad \hat{\alpha} = 0, \\ E_1(\hat{\alpha}\tau_1) - E_1(-\hat{\alpha}\sigma_+) &= \eta \quad \text{for} \quad \hat{\alpha} < 0. \end{aligned} \right\} \quad (106)$$

(There is no singularity of $\hat{\alpha}$ in (105) since $T_\infty - M_0^2 V_\infty$ is positive for $0 \leq M_0 < M_{0c}$, as is easily shown.)

REFERENCES

1. Buckmaster, J. & Ludford, G.S.S. 1981. Theory of Laminar Flames, Cambridge University Press.
2. Buckmaster, J. 1976. The quenching of deflagration waves. Combust. Flame. 26, 151-162.
3. Bush, W.B. & Fendell, F.E. 1970. Asymptotic analysis of laminar flame propagation for general lewis numbers. Combust. Sc. Tech. 1, 421-428.
4. Liñán, A., 1974. The asymptotic structure of the counterflow diffusion flames for large activation energy. Acta Astronaut. 1, 1007-1039.
5. Lu, G.C. & Ludford, G.S.S. 1980. Asymptotic analysis of plane steady detonations. Submitted for publication.
6. Spalding, D.B. & Yumlu, V.S. 1959. Experimental demonstration of the existence of two flame speeds. Combust. Flame. 3, 553-556.

TABLE 1

γ	Ratio of specific heats
M_o	Mach number of flame with respect to undisturbed speed of sound
Pr	Prandlt number
Le	Lewis number
α	Nondimensional heat of reaction
θ	Activation energy
D	Damköhler number
Λ	$= DM^{-2}$

Captions:

Fig. 1a. M_0^2 versus T_* for $Pr = 1$, $Le = 1$, $\gamma = 5/3$, $\beta = .5$, $T_a = 1.5$

where $M_{OCJ}^2 = .225$.

Fig 1b. M_0^2 versus t_* for $Pr = 1$, $Le = 1$, $\gamma = 5/3$. Dashed line for $\beta = .09$ where $M_{OCJ}^2 = .51$. Solid line is the asymptotic result (34).

Fig. 2a. Leading-order profiles of velocity, temperature, pressure and mass fraction for $Pr = 1$, $Le = 1$, $\gamma = 5/3$, $\beta = .5$, $M_0^2 = .2$ corresponding to $T_* = 1.43$.

Fig. 2b. Pressure profiles for general Le , $\gamma = 5/3$, $M_0^2 = .5$ and various Pr , showing a spike for $Pr > 1$.

Fig. 3. D/m^2 versus T_* for $Pr = 1$, $Le = 1$, $\gamma = 5/3$, $\beta = .09$, $\theta = 50$.

Fig. 4. D/m^2 versus t_* for $Pr = 1$, $Le = 1$, $\gamma = 5/3$, $\beta = .5$, $\theta = 50$.

Fig. 5. M_0^2 versus D/m^2 for fast and very slow deflagrations, $Pr = 1$, $Le = 1$, $\gamma = 5/3$, $\beta = .5$, $\theta = 50$. Drawn for Mach numbers at the upper limit of application of the combustion approximation.

Fig 1a

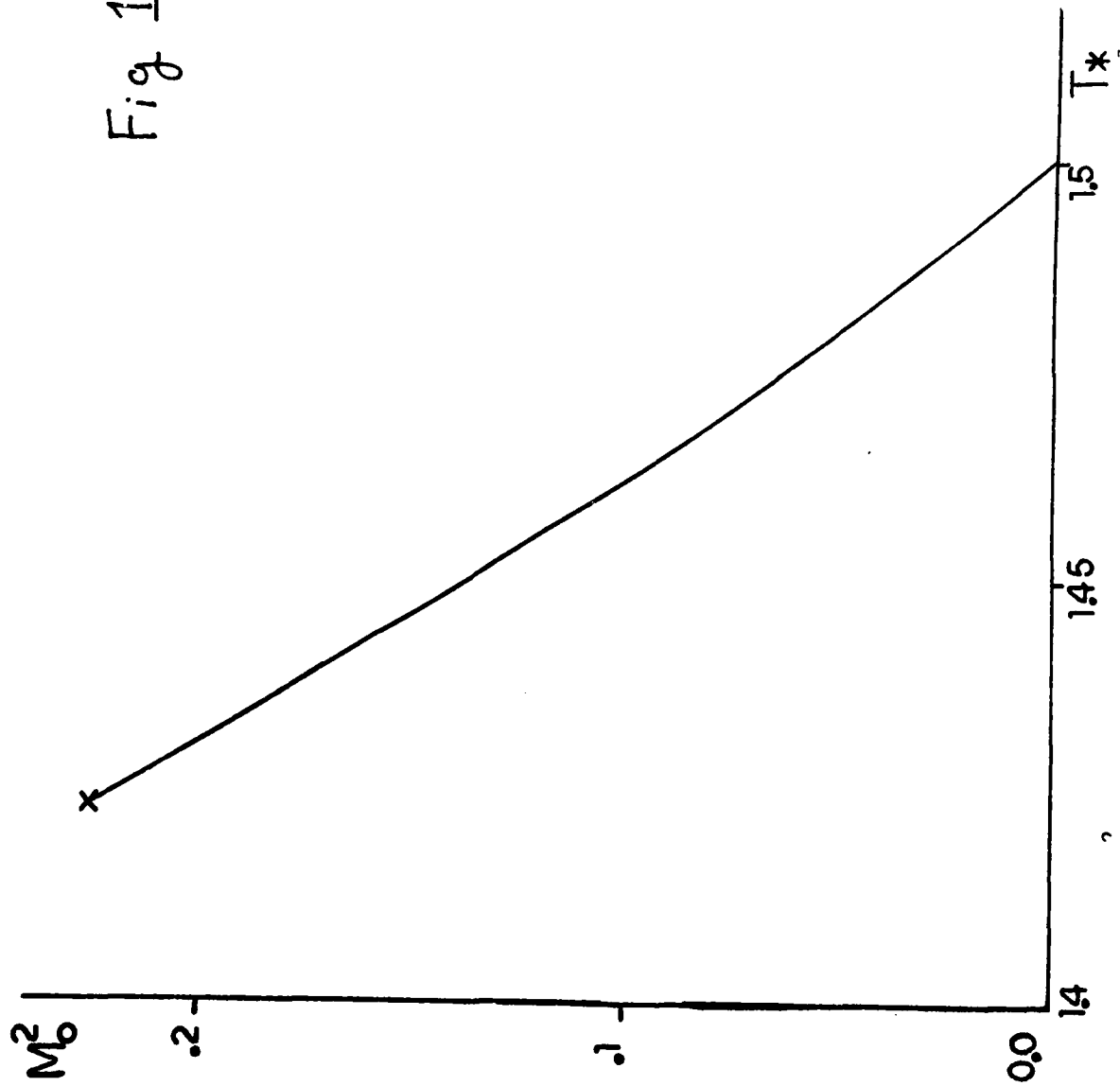


Fig. 16

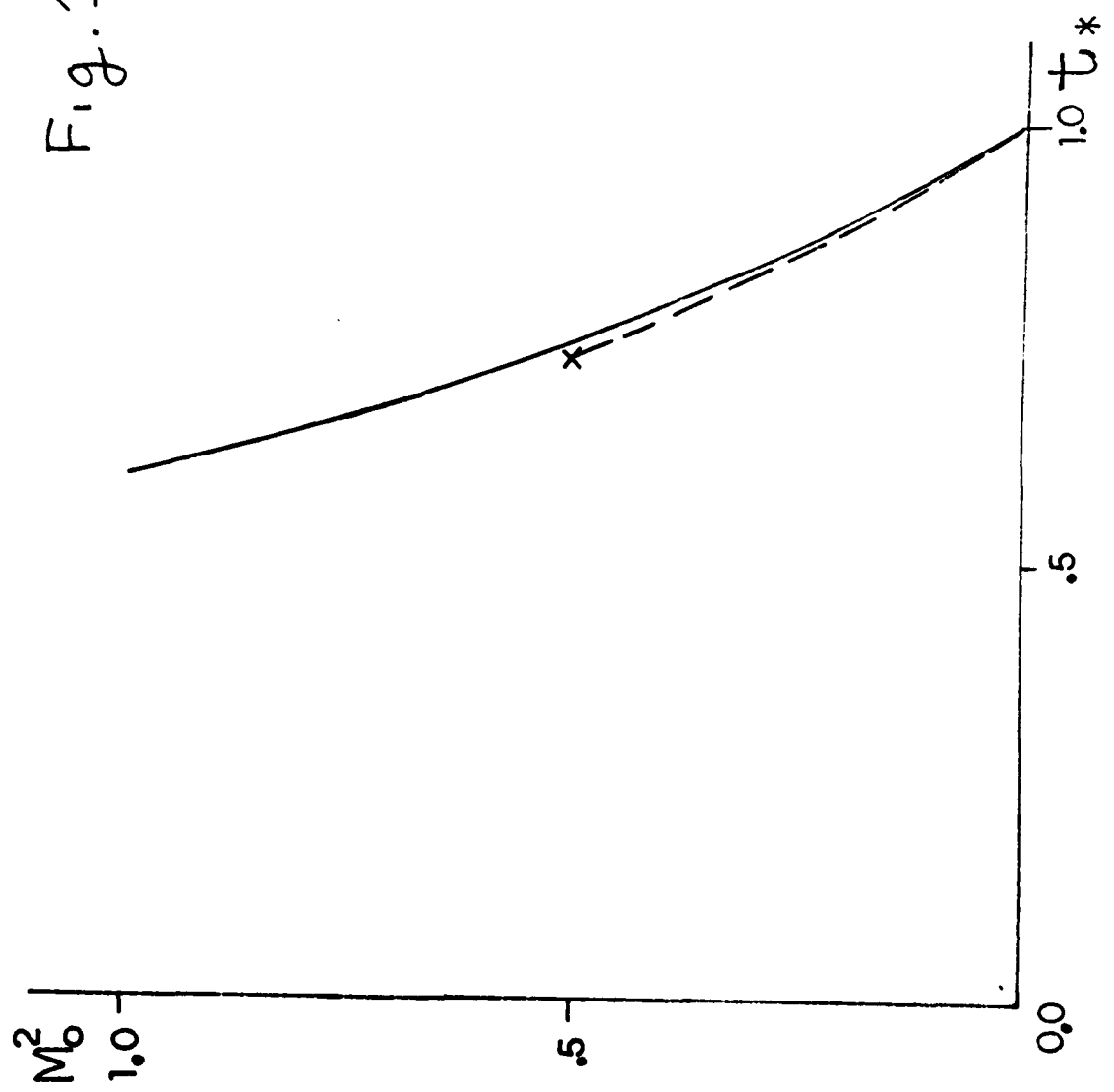


Fig. 2a

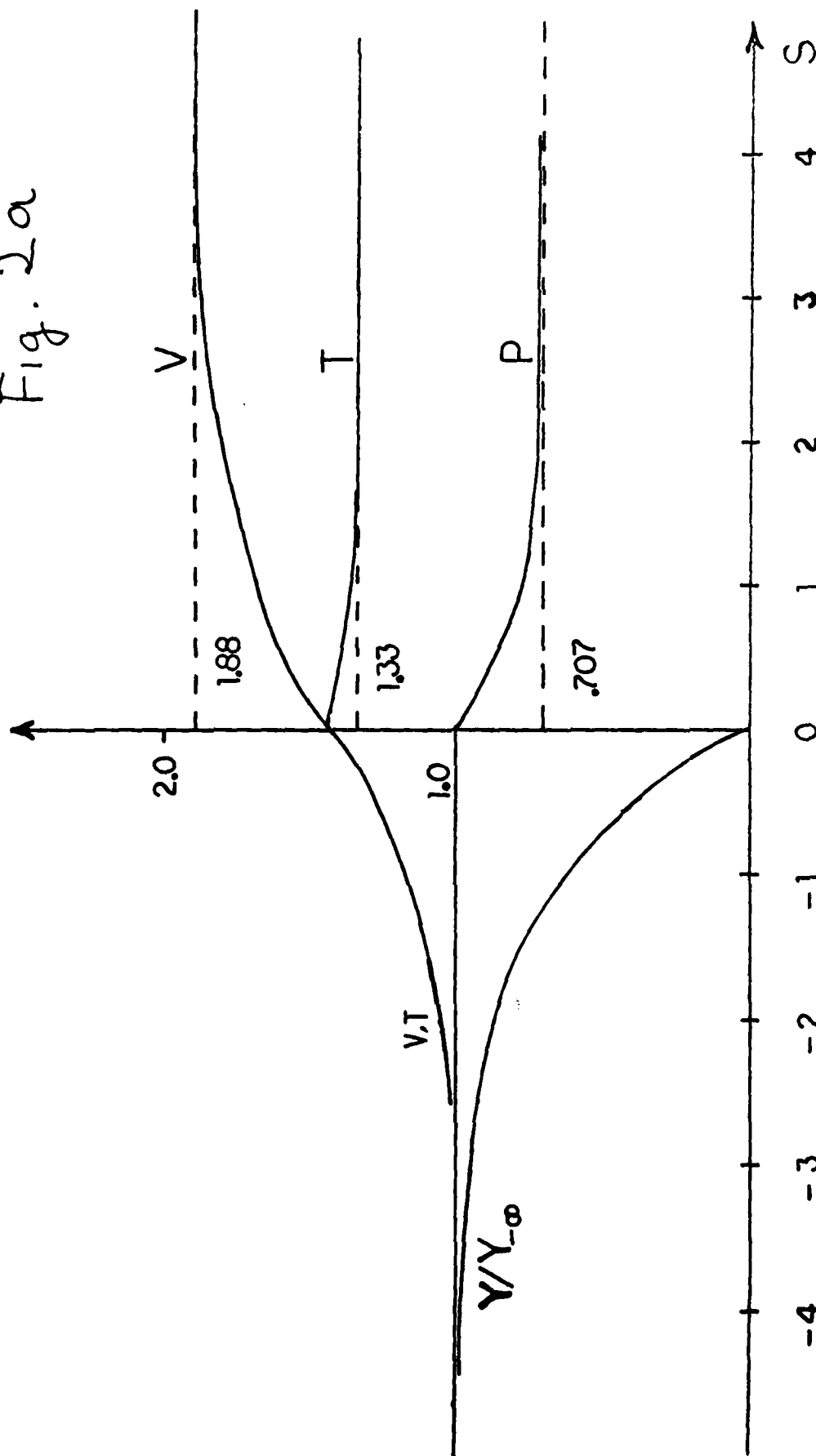


Fig 2b

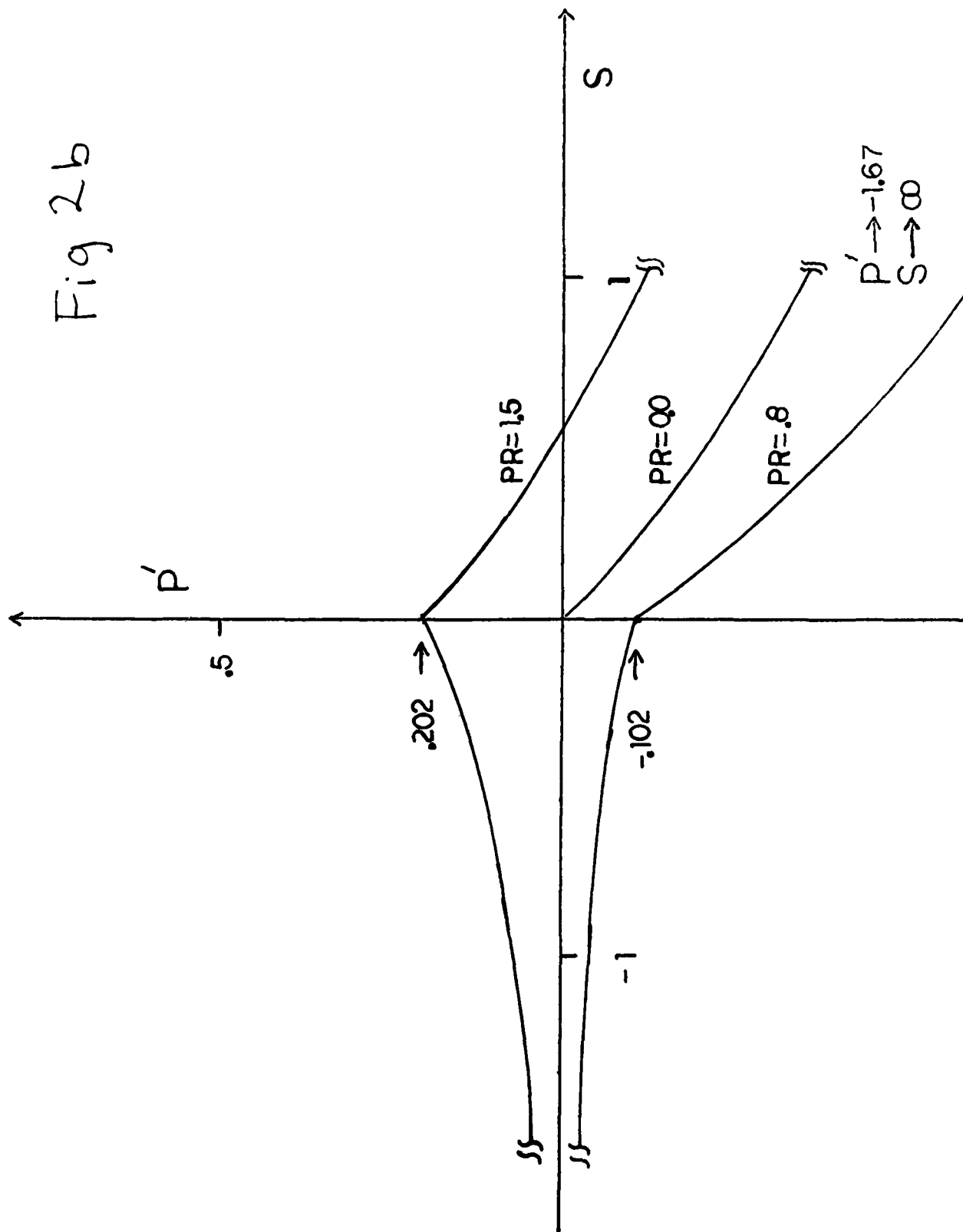
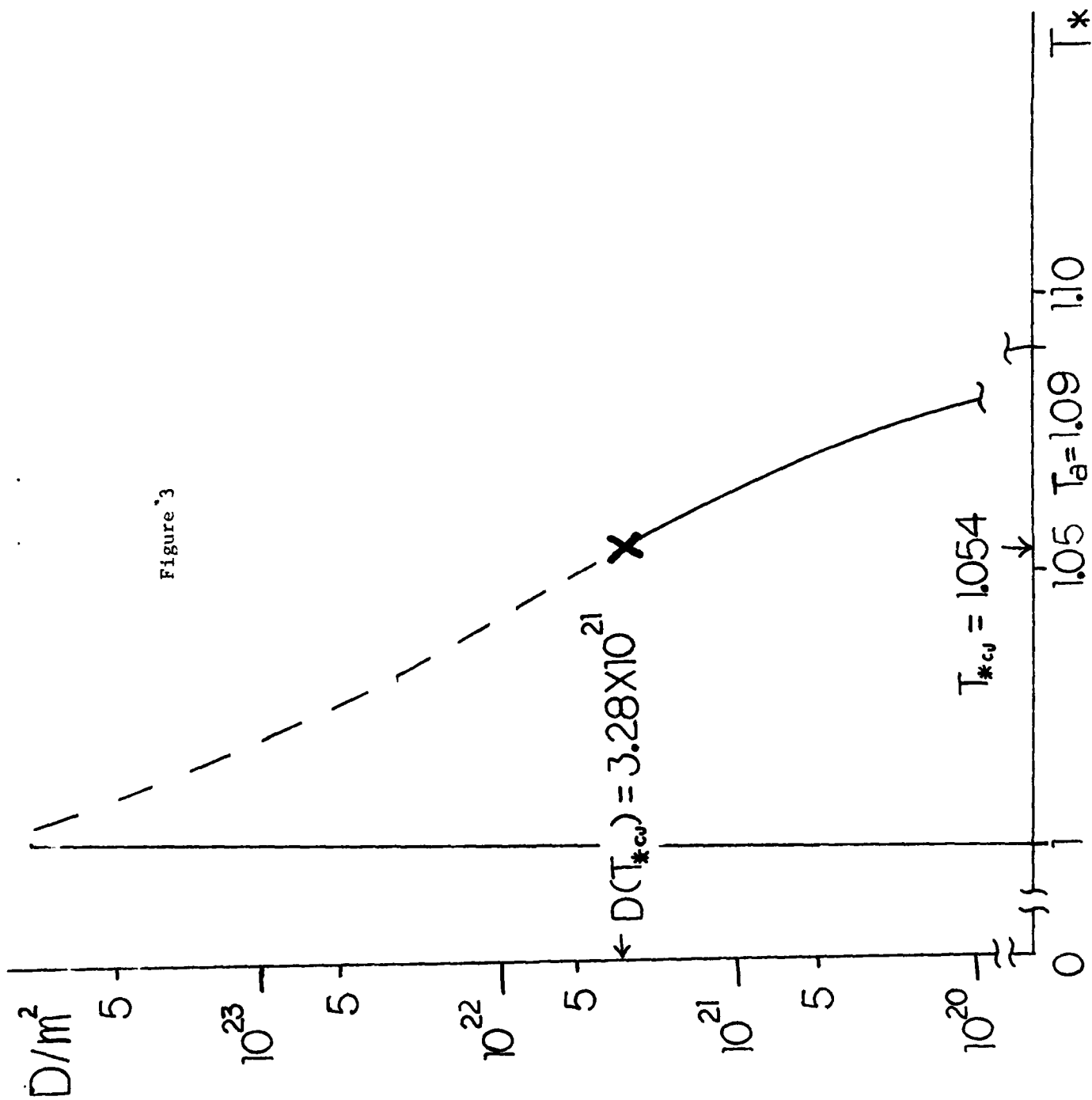


Figure 3



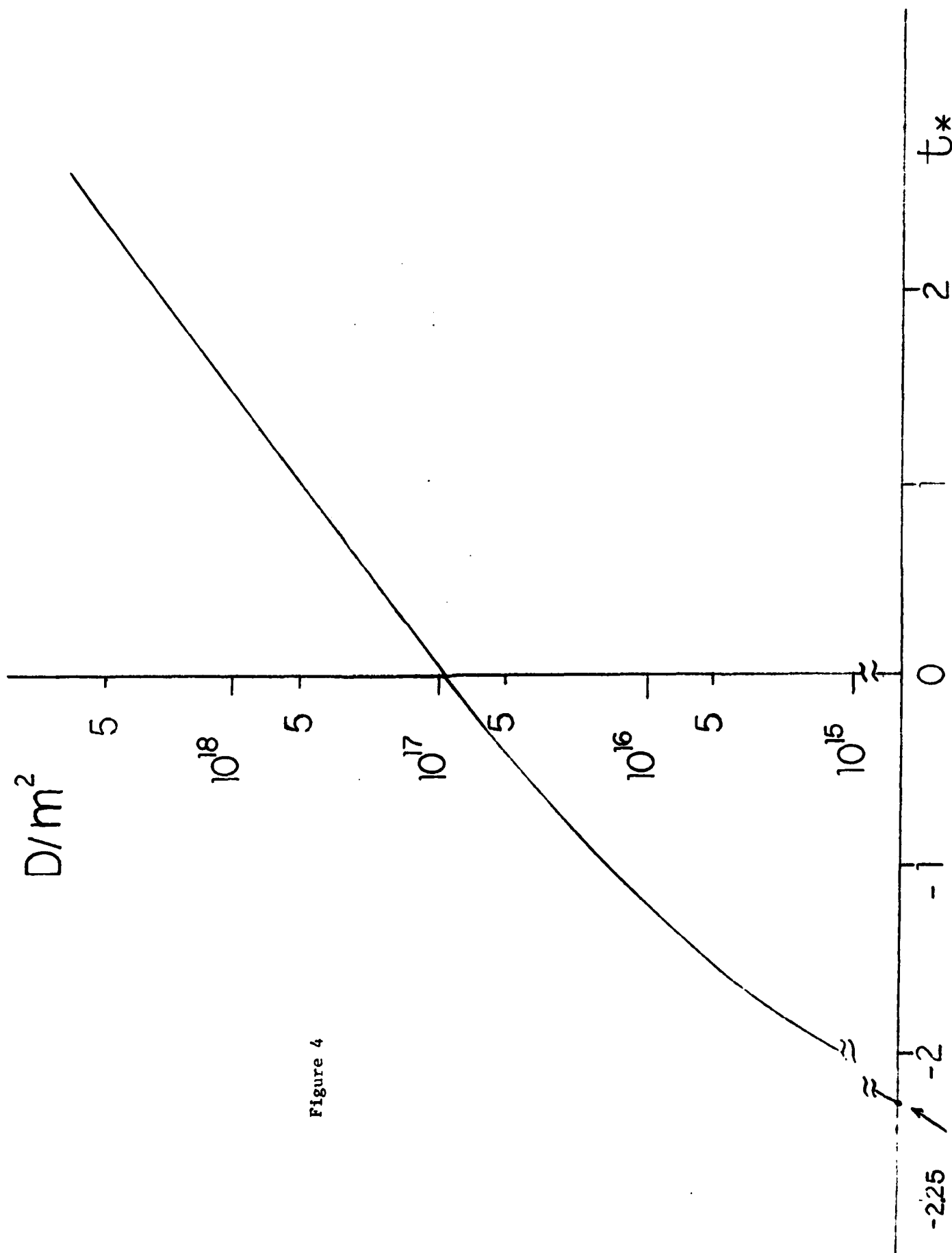
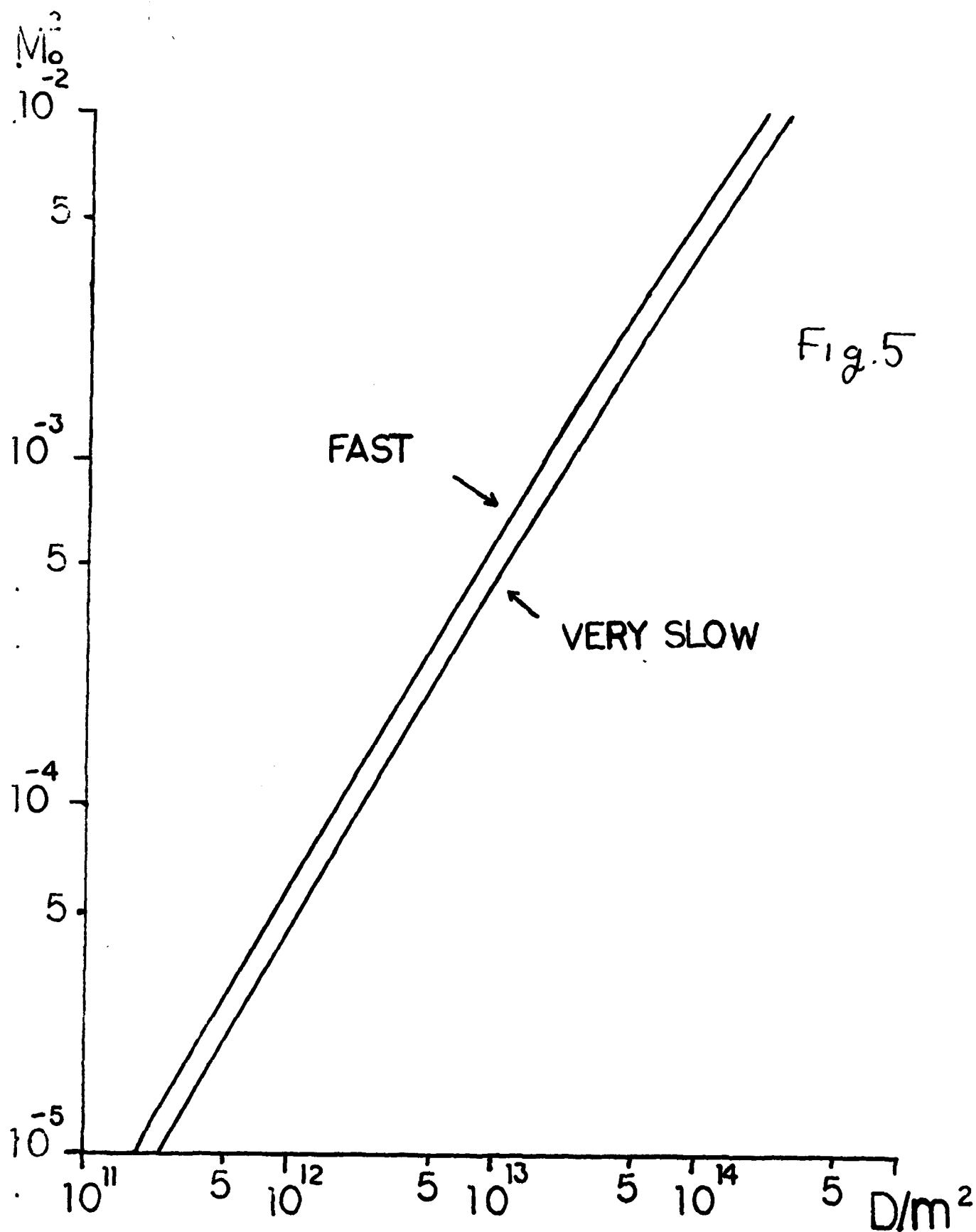


Figure 4



REPORT DOCUMENTATION PAGE		READ INSTRUCTIONS BEFORE COMPLETING FORM
1. REPORT NUMBER 116	2. GOVT ACCESSION NO. AD-A090776	3. RECIPIENT'S CATALOG NUMBER
4. TITLE (and Subtitle) FAST DEFLAGRATION WAVES.		5. TYPE OF REPORT & PERIOD COVERED Interim Technical Report.
7. AUTHOR(s) D.S./Stewart & G.S.S./Ludford		6. PERFORMING ORG. REPORT NUMBER
9. PERFORMING ORGANIZATION NAME AND ADDRESS Department of Theoretical & Applied Mechanics Cornell University, Ithaca, NY 14853		8. CONTRACT OR GRANT NUMBER(s) DAAG29-79-C-0121
11. CONTROLLING OFFICE NAME AND ADDRESS U. S. Army Research Office Post Office Box 12211 Research Triangle Park, NC 27709		10. PROGRAM ELEMENT, PROJECT, TASK AREA & WORK UNIT NUMBERS P-15882-M
14. MONITORING AGENCY NAME & ADDRESS (if different from Controlling Office) 14/TI-11C		12. REPORT DATE July 1980
		13. NUMBER OF PAGES 30
		15. SECURITY CLASS. (of this report) Unclassified
		16a. DECLASSIFICATION/DOWNGRADING SCHEDULE NA
16. DISTRIBUTION STATEMENT (of this Report) Approved for public release; distribution unlimited.		
17. DISTRIBUTION STATEMENT (of the abstract entered in Block 20, if different from Report) NA		
18. SUPPLEMENTARY NOTES The findings in this report are not to be construed as an official Department of the Army position, unless so designated by other authorized documents.		
19. KEY WORDS (Continue on reverse side if necessary and identify by block number) Fast deflagration waves, activation-energy asymptotics, small heat release, combustion approximation, very slow deflagration, exponential tail, deflagration to detonation transition, Mach layer.		
20. ABSTRACT (Continue on reverse side if necessary and identify by block number) The analysis of steady plane deflagration waves invariably starts with the combustion approximation where it is assumed that the Mach number, i.e. the flame speed divided by a characteristic sound speed, is vanishingly small. Even then explicit formulas can only be obtained in the limit of large activation energy. There are circumstances, however, notably the transition from deflagration to detonation, when the Mach number is finite, and the present paper gives a description, again using activation-energy asymptotics, of such fast deflagrations. continued		

404620

JOB

#20 continued.

The main result is a relation between the Mach number and the flame temperature, a parameter determined by the Damköhler number. One of the features of a finite wave speed is the exponentially long tail in which the small amount of reactant escaping the flame front is finally consumed. Another is the velocity adjustment layer which forms behind the flame front as the Mach number becomes small, a layer the combustion approximation cannot detect. Explicit formulas are obtained when the heat release is small; otherwise numerical integration is necessary.

Another class of deflagration waves is uncovered, characterized by Mach numbers that are even smaller than those involved in the combustion approximation. The existence of these very slow deflagrations has been suspected before, but cannot be deduced from the governing equations of that approximation.

For simplicity both the Prandtl and Lewis numbers are taken to be one. The modifications for other values are given in an appendix.